

# Height preference and strain in Ag islands on Si(111)–(7×7) surfaces

D. K. Goswami<sup>1</sup>, K. Bhattacharjee<sup>1</sup>, B. Satpati<sup>1</sup>, S. Roy<sup>1</sup>, G. Kuri<sup>2\*</sup>, P. V. Satyam<sup>1</sup> and B. N. Dev<sup>1†</sup>

<sup>1</sup>*Institute of Physics, Sachivalaya Marg, Bhubaneswar - 751005, India*

<sup>2</sup>*Hamburger Synchrotronstrahlungslabor HASYLAB at DESY, Notkestrasse 85, D-22607, Hamburg, Germany*

(Dated: April 4, 2018)

Growth and strain behavior of thin Ag films on Si substrate have been investigated by scanning tunneling microscopy, cross-sectional transmission electron microscopy and high resolution x-ray diffraction studies. Ag islands formed on Si at room temperature growth show strongly preferred heights and flat top. At low coverage, islands containing two atomic layers of Ag are overwhelmingly formed. At higher coverages island height distribution shows strong peaks at relative heights corresponding to an even number of Ag atomic layers. This appears to be a quantum size effect. Hexagonal disc-like islands with flat top are formed upon annealing. The annealed film shows two closely-spaced Ag(111) diffraction peaks – one weak and broad and the other narrow and more intense. The intense peak corresponds to a shorter Ag(111) planar spacing compared to the bulk value. This can be explained in terms of changes in the Ag lattice during the heating-cooling cycle due to thermal expansion coefficient mismatch between Ag and Si.

PACS numbers: 68.55.Jk, 61.16.Ch, 68.37.Ef, 68.60.Dv

## I. INTRODUCTION

Ag on Si is a nonreactive metal-semiconductor system. The growth of Ag on Si has been widely studied as a model system. Growth morphology has been found to depend on the deposition rate and growth temperature. For Ag deposition on Si(111)–(7×7) at low temperature (LT), reflection high energy electron diffraction (RHEED) oscillations were observed up to many monolayers (MLs) indicating a quasi-layer-by-layer growth [1, 2]. Scanning tunneling microscopy (STM) studies on such samples also indicated quasi-layer-by-layer growth up to 3.6 ML, attributed to a lower average island size and higher island density compared to room temperature (RT) growth [3]. At RT deposition it is generally accepted that the growth follows the Stranski–Krastanov (SK) or layer-plus-island growth mode [4, 5, 6, 7]. However, for RT deposition quasi-layer-by-layer growth has also been observed but only for high deposition rates ( $\sim 30$  ML/min) [1]. An LT growth followed by RT annealing leads to yet another growth mode in which 3D plateaulike Ag islands with a strongly preferred height are observed on a wetting layer [8]. The islands increase their number density and lateral extension with coverage with no change in height, eventually forming a percolated network of the same preferred height. This behavior was observed where 1 ML to a maximum of 2.2 ML deposition was studied [8]. This growth mode is different from the conventional SK growth mode. The role of electronic driving force has been suggested to be responsible for this mode of growth. Zhang and coworkers proposed the *electronic growth* mechanism, in which uniform layer can be grown

only over a thickness window, below or above which the metal film would be nonuniform [9, 10]. According to their work, very thin films are destabilized by charge transfer at the interface, films of intermediate thickness are stabilized by quantum confinement and thick films are destabilized by stress. Huang et al studied Ag growth on Si(111)–(7×7) at 50 K followed by annealing at 300 K [11]. By STM measurements they observed that flat pin-hole free films can be grown where the amount of material deposited exceeds 6 ML but multilayer pits are observed for thinner films. Growth at 300 K was found to produce three dimensional structures. These authors did not explore much higher film thicknesses to find out if there exists a thickness window above which the film again becomes nonuniform. To explore this aspect films of higher thicknesses are to be studied. The authors of ref. [11] studied only a maximum thickness of 6.4 ML. Moreover, at RT growth whether plateaulike islands with a strongly preferred height are formed, as observed by Gavoli et al. [8] for LT deposition and RT annealing, has not been explored. In their study the thinnest Ag film on Si(111)–(7×7) grown at 300 K was 5 ML. Thinner films are to be studied to reveal any plateaulike islands with a height preference.

Here we report on our studies of growth of Ag films over a wide range of thickness on Si(111)–(7×7) surfaces for RT growth as well as RT growth plus annealing at higher temperatures by STM, transmission electron microscopy (TEM) and high resolution x-ray diffraction (HRXRD) experiments. Encouraged by the fact that for other metal/Si systems LT [12] as well as RT [13] deposition shows growth of islands with preferred heights as a consequence of quantum size effect (QSE), we explore whether a height preference exists for the growth of Ag on Si over a range of thicknesses for RT growth. Indeed we observe growth of plateaulike Ag islands with an N-layer (N even) height preference. These aspects alongwith the detailed morphology and strain in annealed films are pre-

\*Present address: Paul Scherrer Institute, CH-5232 Villigen PSI, Switzerland.

†Electronic address: bhupen@iopb.res.in

sented here.

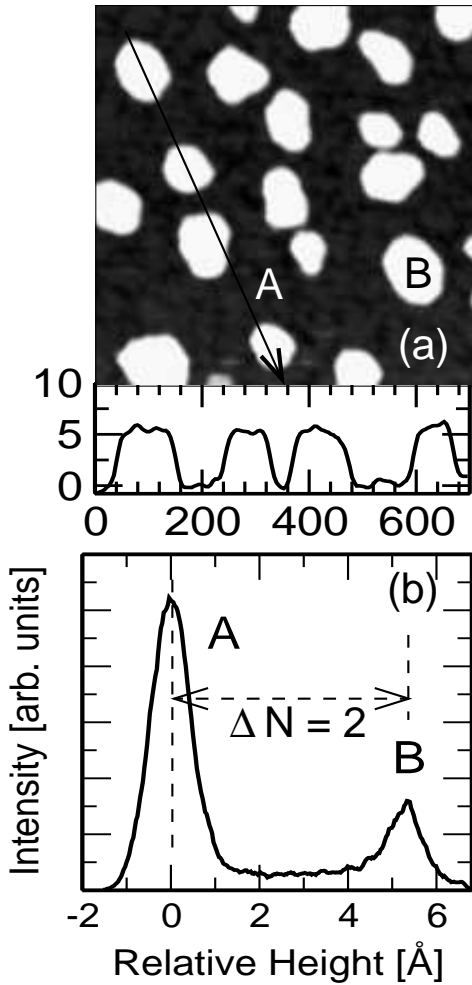


FIG. 1: (a) STM image ( $700 \times 700 \text{ \AA}^2$ ) of a 1 ML Ag film deposited on a Si(111)-(7 $\times$ 7) surface at RT. Sample bias voltage  $V_s = 2.1 \text{ V}$ , tunneling current  $I = 0.2 \text{ nA}$ . Height profile along the line is shown (scales are in  $\text{\AA}$ ) (b) Island height distribution obtained from the image in (a), showing the strongly preferred height (peak B) corresponding to two atomic layers of Ag(111). Peak A represents the Ag wetting layer.

## II. EXPERIMENTAL DETAILS

Growth and STM measurements were performed in a custom made molecular beam epitaxy (MBE) chamber coupled with an ultrahigh vacuum (UHV) variable temperature scanning tunneling microscope (VTSTM, Omicron). This system has been described elsewhere [14]. Base pressure in the growth chamber was  $1 \times 10^{-10}$  mbar. Si(111) samples were cut from n-type silicon wafers with resistivity in the range 10–20  $\Omega\text{cm}$ . After introducing into the MBE chamber, substrates were degassed at  $600^\circ\text{C}$  for about 12 hours. The sample was then flashed briefly at  $1150^\circ\text{C}$  to remove the native oxide and

cooled slowly to RT. The (7 $\times$ 7) reconstruction was observed on Si(111) surface by STM. Ag was evaporated from a Knudsen cell (PBN crucible) and deposited onto the Si(111)-(7 $\times$ 7) surfaces, kept at RT, at the rate of 2 ML/min. (Some authors have defined a monolayer of Ag to be equivalent to the normal surface atomic density of Ag(111), which is  $1.5 \times 10^{15}$  atoms/cm $^2$ . Others have defined a monolayer to be the equivalent of the atomic density on an ideal Si(111) surface, which is  $0.78 \times 10^{15}$  atoms/cm $^2$ . Here we use the former definition). For the annealed samples, annealing was performed following deposition in the MBE chamber. During deposition the chamber pressure rose to  $8.5 \times 10^{-10}$  mbar. The sample was then transferred into the VTSTM chamber for microscopy measurements at RT. Following STM measurements samples were taken out of the UHV chamber for HRXRD and TEM measurements. Film thickness was measured during growth by a quartz microbalance as well as post-growth Rutherford backscattering spectrometry (RBS) experiments. HRXRD measurements with a rotating anode source and TEM measurements with a JEOL-2010 microscope using 200 keV electrons were made in Institute of Physics. HRXRD measurements were also performed with synchrotron radiation at HASYLAB at DESY in Germany at the bending magnet beamline ROEMO-I.

For HRXRD measurements with a rotating anode source, we have used Mo  $K_{\alpha 1}$  X-rays ( $\lambda = 0.709 \text{ \AA}$ ) monochromatized by a symmetrically cut Si(111) crystal. For experiments with synchrotron radiation (SR) a pair of symmetrically cut Ge(111) crystals were used in a double-crystal monochromator. A beam entrance slit (S1: vertical opening  $70 \mu\text{m}$ , horizontal opening 0.5 mm) 46 cm before the sample and another slit (S3: vertical opening  $200 \mu\text{m}$ ) before the detector at a distance of 43 cm from the sample were used. An antiscattering slit (S2: vertical opening  $80 \mu\text{m}$ ) was used between the sample and the entrance slit. During sample alignment smaller vertical opening of the slits were used (S1:  $30 \mu\text{m}$ , S3:  $100 \mu\text{m}$ ). X-rays of a longer wavelength ( $\lambda = 1.033 \text{ \AA}$ ) were used for the SR experiments.

## III. RESULTS AND DISCUSSIONS

### A. Growth and morphology

For a thin (1 ML) Ag layer grown on a Si(111)-(7 $\times$ 7) surface at RT, a STM image is shown in Fig.1(a). A height scan along the line marked in Fig.1(a) is shown below the image. Growth of flat-top islands with a preferential height is evident from the height scan. Indeed all the islands seen in Fig.1(a) have the same height. Height distribution of Ag islands obtained from the micrograph in Fig.1(a) is shown in Fig.1(b). The dark background area (marked 'A') in Fig.1(a) corresponding to peak A in Fig.1(b) is the first Ag wetting layer on Si(111). The bright features (marked 'B') in Fig.1(a) corresponding to

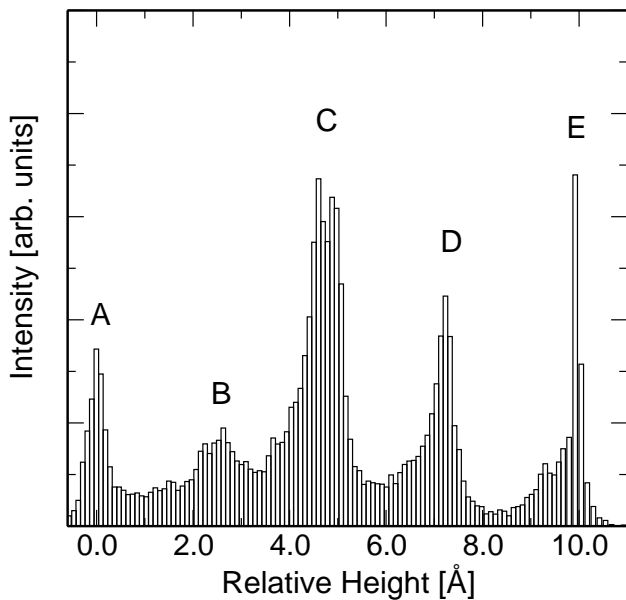


FIG. 2: Height distribution obtained from a STM image of a 2 ML Ag film. Peak A corresponds to the wetting layer and B, C, D and E correspond to islands of monolayer, bilayer, trilayer and quadrilayer heights, respectively. Islands of double-layer and four-layer heights are dominant.

peak B in Fig.1(b) are Ag islands with flat top and a height of 5.4 Å from the Ag wetting layer. Assuming that the spacing between atomic layers in the Ag islands is close to the corresponding value in bulk Ag along the [111] direction, each island contains two atomic layers of Ag. The wetting layer contains about 0.5 ML Ag [8], the remaining deposited Ag grows as islands on the wetting layer. So the double-layer height preference of the Ag islands is obvious. This height preference of Ag islands for RT growth of Ag on Si(111)-(7 × 7) surfaces is quite robust. Among several STM images, in one image similar to Fig.1(a), among islands of double-layer height only one island of a height corresponding to three atomic layers of Ag was found. We observed no Ag islands of one atomic layer height. The root-mean-square roughness on any given island is  $\sim 0.2$  Å while that obtained from the whole image [Fig.1(a)] is 2.2 Å. The double-layer height (5.4 Å) preference of Ag islands for the Ag/Si(111)-(7 × 7) system was earlier observed only for LT (150 K) deposition followed by RT (300 K) annealing for deposition between 1 and 2.2 ML Ag [8].

This novel growth mode was qualitatively explained in terms of the *electronic growth* mechanism [9, 10], wherein the quantized electrons in a layer can influence the morphology. As we observe here, for the Ag/Si(111) system LT growth followed by RT annealing is not a necessary condition for the formation of islands of preferred heights. They are also formed in RT deposition. Moreover, height preferences with larger heights have been observed in other metal/silicon systems [12, 13]. We investigated growth of Ag layers of various thicknesses (1–60 ML).

For 2 ML Ag films preference for growth of islands of N-layer ( $N \geq 2$ ) height is observed. A height distribution plot obtained from a STM image of a 2 ML film is shown in Fig.2. There is a strong tendency of height preference in units of bilayer height [ $N = 2$  (A–C), 4 (A–E)]. From Fig.2 we also notice the existence of monolayer B and trilayer D heights; however, their intensities are smaller. The monolayer height peak B arises from the height difference between C and D, i.e., growth of monolayer height islands on the already formed double-layer height islands. Direct growth of monolayer height islands on the wetting layer A is very rarely observed. For the growth of 4 ML onwards, the Ag layer forms a percolating structure. The

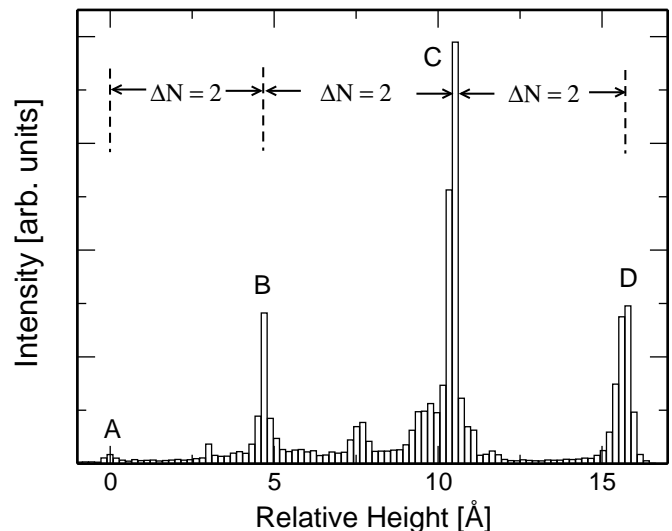


FIG. 3: Height distribution obtained from a STM image ( $350 \times 850 \text{Å}^2$ ) of a 5 ML Ag film. N-layer heights of islands (B:  $N = 2$ , C:  $N = 4$ , D:  $N = 6$ ) for even values of N are strongly preferred.

height distribution from a 5 ML Ag film is shown in Fig.3. Growth of islands of N-layer ( $N$  even: 2, 4, 6) height is prominent. The peaks A, B, C, D in Fig.3 correspond to the wetting layer,  $N = 2$ ,  $N = 4$ ,  $N = 6$  islands. These heights are seen in line scans through the STM image (not shown). STM images from 20 ML, 30 ML and 40 ML Ag films are shown in Fig.4. The roughness obtained from the STM image in Fig.4(c) is 6.2 Å, while that only on the flat features is  $\sim 0.2$  Å. Small hexagonal islands appear to grow on the outer layers beginning around 30 ML thick films. These hexagonal islands become more prominent for 40 ML and 60 ML (shown later) films. Height distribution in the 40 ML film is shown in Fig.5. Height preference for even-N is observed. Peak A in Fig.5 is not from the wetting layer. The wetting layer has been covered by further growth on it. If we assume the height corresponding to A to be  $N_0$ -layer then we observe strong preference for  $N_0+2$ ,  $N_0+4$  and  $N_0+6$  layers in Fig.5. These heights can be appreciated from the height scan and the grey scale in the marked area in Fig.4(c). Apparently the N-layer height preference with an even value

of  $N$  is an effect of quantum confinement of electrons in the Ag islands. To our knowledge in the existing literature neither theoretical nor experimental results (except for  $N = 2$  in LT growth followed by RT annealing [8]) on the height preference in Ag(111) films on Si(111) sub-

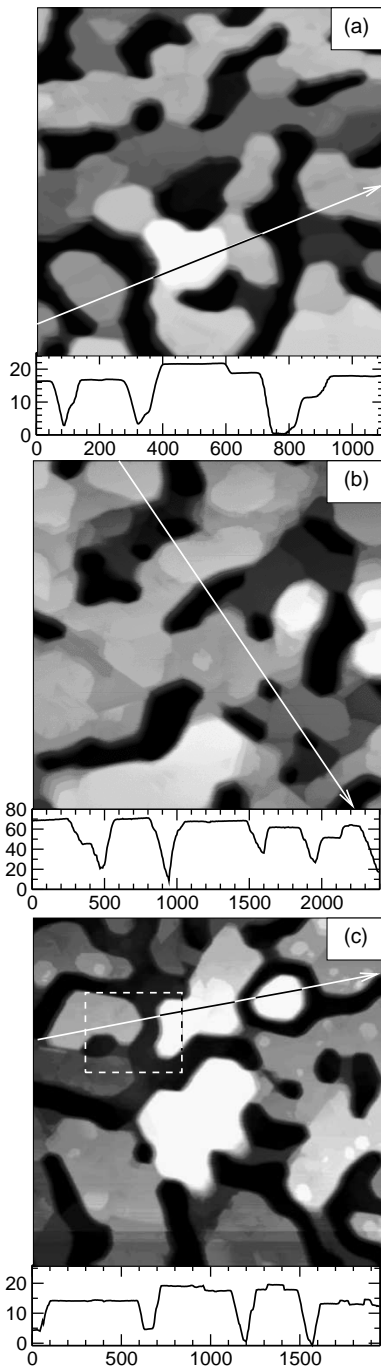


FIG. 4: STM images of (a) 20 ML ( $1000 \times 1000 \text{ \AA}^2$ ), (b) 30 ML ( $2000 \times 2000 \text{ \AA}^2$ ) and (c) 40 ML ( $2000 \times 2000 \text{ \AA}^2$ ) Ag films. Height profiles along the marked lines are shown (scales are in  $\text{\AA}$ ). Small hexagonal islands on the top layer begins to grow for  $\gtrsim 30$  ML films. These islands are more abundant on 40 ML films.

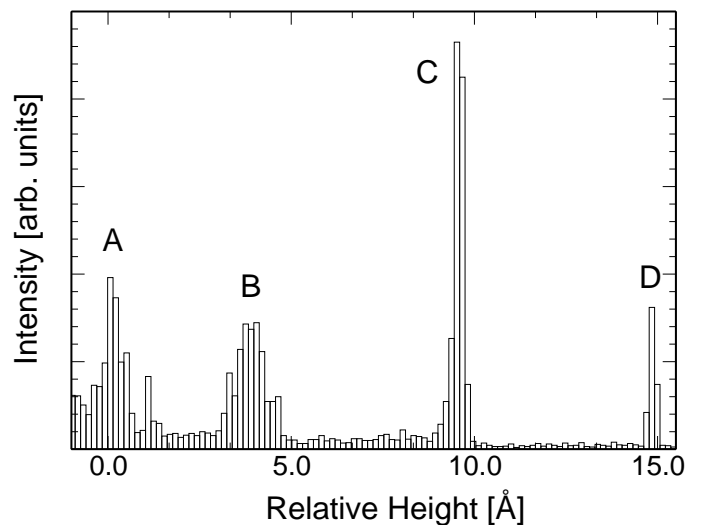


FIG. 5: Height distribution obtained from the marked area with dashed lines in Fig. 4(c). Relative heights apparently correspond to A–B:  $\Delta N = 2$ , A–C:  $\Delta N = 4$ , A–D:  $\Delta N = 6$ . Here the peak A does not correspond to the wetting layer. Relative height for a given  $\Delta N$  may somewhat depend on the value of  $N$  ( see text for details).

strates are available. Recently for Pb islands grown on Si(111) substrates, Okamoto et al. observed a preference for islands with height differences ( $\Delta N$ ) equivalent to an even number of Pb atomic layers [13]. Surface energy has been found to be lower for a height containing an even number of atomic layers, compared to the neighboring heights containing an odd number of layers. For Ag films on Fe(100) surfaces, in general an  $N$ -layer film, though stable at low temperature, was found to bifurcate into a film with  $N \pm 1$ , i.e.  $\Delta N = 2$ , around 400 K [15]. Some theoretical attempts have been made to understand the  $N$ -dependent stability of metal films using the quantization condition (the phase accumulation model):

$$2k_z(E)Nd_0 + \phi_1(E) + \phi_2(E) = 2n\pi \quad (1)$$

where  $k_z$  is the component of the wave vector perpendicular to the film surface,  $k_z(E)$  is determined by the band structure,  $d_0$  is the interlayer spacing and  $n$  is an integer.  $\phi_1(E)$  and  $\phi_2(E)$  are the energy-dependent phase shifts of the electronic wave function upon reflection at the two boundaries of the film [16]. For the Ag(111)/Si(111) case this would depend on the Ag band structure (energy dispersion along [111] direction) and the phase shifts at Ag/vacuum and Ag/Si interfaces. Although for a direct comparison, calculation for the Ag/Si(111) system would be necessary, it is evident that quantum size effect (QSE) is important in leading to the observed height preference of Ag islands.

It is interesting to note that the bilayer height on the wetting layer for the thinnest Ag film (1 ML) is about  $5.4 \text{ \AA}$  (Fig.1). (The same value of the double-layer height

was observed by Gavioli et al.[8] for film thicknesses between 1 and 2.2 ML. These authors did not study thicker films). However, for the thicker films (see figures 2, 3 and 5) we observe some variation in the bilayer separation. [It should be noted that the actual value depends somewhat on the magnitude of the sample bias voltage and its sign. However, the trend remains the same]. While for Ag islands on Si no report is available on thickness relaxation depending on the total number of atomic layers in an island, for Pb islands on Si(111) surfaces an oscillatory thickness relaxation was observed depending on the number of atomic Pb layers in the islands. This oscillatory thickness relaxation has been shown to be correlated with quantized electronic states in the Pb islands [12]. The thickness relaxation has been characterized in terms of the deviation from ideal thickness, defined as  $\Delta t = t_N - Nd_0$ , where  $N$  is the number of atomic layers on the wetting layer,  $d_0$  is the ideal interlayer spacing and  $t_N$  is the thickness of the island. For small  $N$  the deviations were found to be large [for example,  $\Delta t = -0.5\text{\AA}$ ,  $0.2\text{\AA}$  and  $-0.4\text{\AA}$  for  $N = 5$ ,  $N = 6$  and  $N = 7$  respectively]. The amount of deviations also apparently depend on whether the islands are isolated individual islands or islands of several tiers. (For Ag islands we show the characteristic differences for these cases later). With increasing thickness the island height variation tends to diminish.

For as-deposited 60 ML films, growth of hexagonal islands is prominent as seen in the STM image of Fig.6. A height scan along the line in Fig.6(a) across multi-tier islands is shown in Fig.6(b). Single-layer height at the island edges are preferred. It is seen from Fig.6(b) that step heights for the inner layers are  $\sim 2.6\text{\AA}$ , while those of the outer layers are  $\sim 3\text{\AA}$  – both much larger than the ideal Ag(111) layer spacing ( $2.36\text{\AA}$ ). [It should be noted that height measurement by STM is affected by both structural and electronic contribution]. As we will show later for annealed samples, where both individual and multi-tier islands are observed, multi-tier island edges prefer single-layer height (like that in Fig.6) whereas individual islands prefer double-layer or in general even-layer height. This trend has also been observed for Pb islands on Si(111), where  $N$  values, which are practically absent in isolated islands, are observed for multi-tier islands showing monolayer steps [12].

In the standard SK growth in RT deposition for film thicknesses above the wetting layer, formation of 3D multilayer Ag islands have been observed [6]. Here in RT deposition for thin Ag films (1 ML) we have observed formation of 3D Ag islands with flat top and a strong preference for a double-layer height. Growth of 3D Ag islands with a flat top and a preferred double-layer height was earlier observed only for 1–2.2 ML Ag films deposited at LT (150 K) followed by annealing at RT (300 K). For RT deposition this feature of Ag island growth on Si with a height preference has not been reported earlier. However, for Pb islands on Si(111), island height preference indicating quantum size effect was observed for growth at

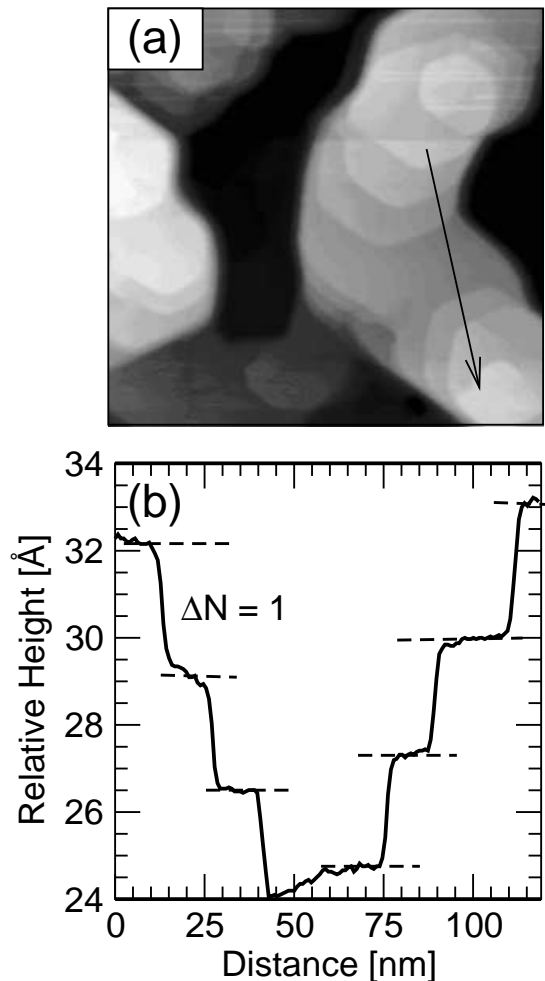


FIG. 6: (a) STM image ( $3000 \times 3000\text{\AA}^2$ ) of an as-deposited 60 ML Ag film. Multi-tier islands, present but not prominent on the 40 ML film, are very prominent here. (b) a height scan along the line in (a). Monolayer ( $\Delta N = 1$ ) steps are found to be dominant for these multi-tier islands.

170–250K [12], 273K [17] and even at RT [13]. For higher film thicknesses (4 ML onwards), we observe the growth of a percolated Ag layer with a flat top feature on the islands with a height preference in units of double-layer height.

The RT-deposited 40 ML film, when annealed at  $700^\circ\text{C}$ , nanostructural hexagonal disc-like Ag islands are formed as seen in the STM micrograph of Fig.7(a). [Very few hexagonal islands appear in the as-deposited film (compare Fig.4(c))]. According to kinetic Monte Carlo simulation results, islands can grow on a substrate of threefold symmetry in various shapes depending on growth temperature – hexagonal shape being one of them [18]. We have also observed triangular island growth in a Ag film on Si(111) annealed at  $600^\circ\text{C}$  [14]. A height scan along the line in Fig.7(a) is shown in Fig.7(c). We notice that the hexagonal disc-like Ag islands have a preference for a height difference, where  $\Delta N$  is even. This appears to be the case when the islands are individual islands. How-

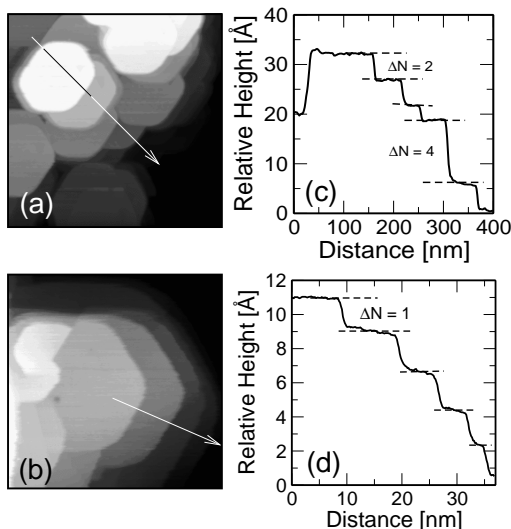


FIG. 7: STM images (a, b) of a 40 ML Ag film annealed at  $700^{\circ}\text{C}$ . Prominent hexagonal disc-like islands are seen to have been formed. There are significant differences in the islands in (a) and (b). In (a) islands are apparently independent islands while in (b) smaller islands on progressively larger islands in a multi-tier form are seen. (c) Height scan along the line in (a) shows strong preference for height differences corresponding to an even number of Ag atomic layers. (d) Height scan along the line in (b) shows monatomic height on the island edges similar to what is seen in Fig.6 for multi-tier islands. Note the large difference in lateral dimensions in (a) and (b). Individual hexagonal islands are much larger.

ever, when the islands are multi-tier islands, i.e. small islands growing on larger islands, the edges prefer to have monolayer steps, as seen in Fig.7(b) and its corresponding height scan in Fig.7(d). Differences between individual and multi-tier islands have also been observed for Pb islands on Si(111)-(7 × 7) surfaces [12], although for much thinner films. For the Ag films of Si(111), up on annealing, growth of individual islands with  $\Delta N = 2$  or 4 becomes more prominent compared to multi-tier islands with  $\Delta N = 1$ . This indicates that  $\Delta N = 2$  or 4 is energetically more favorable. For Pb islands on Si(111) as well, up on annealing  $\Delta N = 1$  tends to disappear in favor of  $\Delta N = 2$  islands [12]. For Pb/Si(111) this has been attributed to quantum size effect. For Ag/Si(111) theoretical results would be necessary for a direct comparison.

Within our limited search over selected thicknesses (1, 2, 4, 5, 10, 30, 40 and 60 ML) we have not observed uniform film growth. An extended search would be necessary to explore if there at all exists a thickness window over which film of uniform thickness can grow at RT or any other growth temperature.

## B. Strain

High resolution x-ray diffraction (HRXRD) measurements were made with a rotating anode X-ray source (Mo

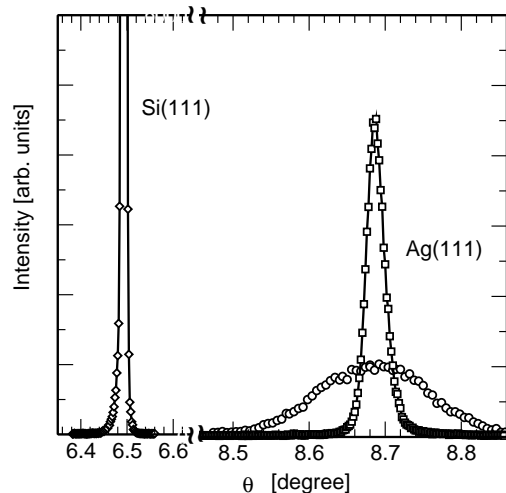


FIG. 8: X-ray diffraction data obtained from 40 ML Ag films with x-rays of  $\lambda = 0.709 \text{ \AA}$  from a rotating anode source (circle: as-deposited film, square:  $700^{\circ}\text{C}$ -annealed film). Epitaxy of Ag(111) layer improves up on annealing as the narrowing of the Ag(111) peak indicates.

$K_{\alpha 1}$ ,  $\lambda = 0.709 \text{ \AA}$ ) on the Ag layers. Typical HRXRD results ( $\theta$ - $2\theta$  scan) from a 40 ML Ag film are shown in Fig.8. Epitaxial growth of Ag(111) layer is seen from the Ag(111) diffraction peak. No other Ag peaks were observed. The diffraction peak from the as-deposited film is broad, which can be attributed mainly to a mosaic spread. Mosaic spread in Ag(111) layers deposited on Si(111) at RT has been observed earlier [20, 21]. Mosaic spread decreases upon annealing. HRXRD results from a Ag layer annealed at  $700^{\circ}\text{C}$  (30 min.) shows a much narrower Ag(111) peak indicating a reduction of mosaic spread and improvement of epitaxy upon annealing. The Ag film, annealed at  $700^{\circ}\text{C}$ , as mentioned before, form hexagonal disc-like islands (see Fig.7). Much thicker Ag islands are formed in this annealed sample. TEM measurements reveal this feature. Typical cross-sectional TEM micrographs and a transmission electron diffraction pattern are shown in Fig.9. The island in Fig.9(a) is  $\sim 500 \text{ \AA}$  thick – more than five times the deposited nominal thickness. The selected area diffraction pattern taken from the region shown in Fig.9(a) shows diffraction from both Si and Ag indicating Ag(111)  $\parallel$  Si(111) and Ag[110]  $\parallel$  Si[110]. An isolated Ag island on Si of  $\sim 2000 \text{ \AA}$  thickness is seen in Fig.9(c). In addition to the reduction in mosaic spread in the annealed film, growth of thick islands also may be partly responsible for narrowing of the Ag(111) peak in Fig.8.

HRXRD experiments were also performed on a  $700^{\circ}\text{C}$ -annealed 40 ML film with monochromatized ( $\lambda = 1.033 \text{ \AA}$ ) synchrotron radiation. The result (Fig.10) shows two distinct Ag(111) peaks alongwith the Si(111) diffraction peak. The results in Fig.10 were obtained with  $\theta$ -steps of  $0.002^{\circ}$ . However, we have also verified the authenticity of the Ag double peak structure by repeat-

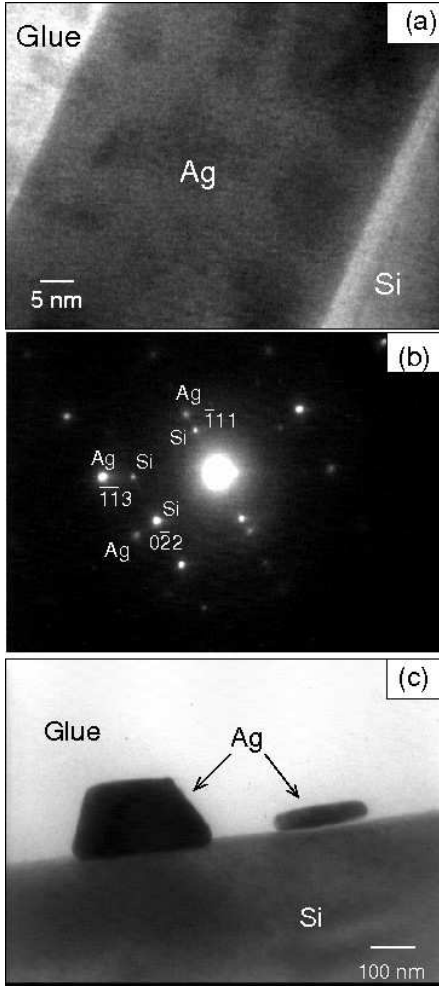


FIG. 9: Cross-sectional TEM micrograph (a) and a transmission electron diffraction pattern (b) from a 40 ML Ag film annealed at 700°C. Epitaxy of Ag(111) with Si(111) is seen from the diffraction pattern. (c) An island about 20 times as thick as the nominal deposited thickness is seen to have formed.

ing experiments with 0.001° steps. The sharp peak and the wide peak correspond to Ag(111) planar spacings of 2.355 Å and 2.364 Å ( $\Delta d = 0.09\text{Å}$ ), respectively ( $\Delta\theta = 0.05^\circ$  between the peaks). The angular positions of the Ag peaks have also been verified with reference to the Si(111) peak position. The sharpness of the peak at larger  $\theta$ , i.e. for  $d=2.355\text{ Å}$  indicates that this component comes from a much thicker layer. As we have seen from Fig.9, much thicker islands, compared to the deposited nominal thickness, are formed in the annealed sample. The broader weak peak apparently comes from thinner islands. The Ag peaks have been fitted using the Takagi-Taupin formalism based on dynamical theory of x-ray diffraction [19]. The theoretical curve for the narrow Ag(111) peak has interference fringes near the base, which are barely visible in this scale.

We now explore the possible origin of the sharp Ag(111) peak corresponding to a shorter planar spac-

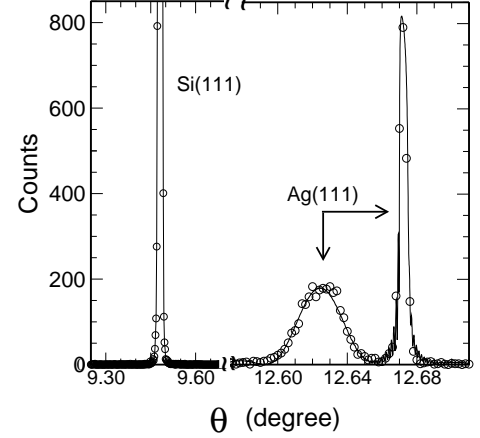


FIG. 10: HRXRD data from a 40 ML Ag film annealed at 700°C, obtained with synchrotron radiation ( $\lambda = 1.033\text{ Å}$ ). Two distinct Ag(111) peaks are observed with a small angular separation  $\Delta\theta = 0.05^\circ$ . The  $d$ -spacing corresponding to the stronger Ag(111) peak is less than that of bulk Ag (see text for explanation). The narrowness of the peak is consistent with the formation of thick islands seen in Fig.9.

ing. Lattice constants of Ag and Si are  $a^{Ag}=4.085\text{ Å}$ , and  $a^{Si}=5.431\text{ Å}$  ( $d_{111}^{Ag}=2.359\text{ Å}$  and  $d_{111}^{Si}=3.136\text{ Å}$ ). The lattice mismatch is  $\sim 25\%$ . However Ag is found to grow epitaxially on Si [20, 21, 22]. This happens via coincidence site lattice matching as  $4a^{Ag} \approx 3a^{Si}$  and the mismatch is just 0.43% ( $4d_{111}^{Ag} > 3d_{111}^{Si}$ ) [22, 23]. In this case an in-plane compression of the Ag layer would lead to a perpendicular strain leading to  $d_{111}^{Ag}(\text{film}) > d_{111}^{Ag}(\text{bulk})$ . However, what we observed is  $d_{111}^{Ag}(\text{film}) < d_{111}^{Ag}(\text{bulk})$  as one component, the other being  $d_{111}^{Ag}(\text{film}) > d_{111}^{Ag}(\text{bulk})$ . A possible explanation for the shorter  $d$ -spacing (2.355 Å) in Ag can be given in terms of coefficients of linear thermal expansion of Ag ( $18.9 \times 10^6/\text{K}$ ) and Si ( $2.6 \times 10^6/\text{K}$ ) [24]. As the expansion coefficient of Ag is about seven times that of Si, the Ag lattice being pinned at the Ag/Si interface would expand faster in the surface-normal direction enhancing strain in the Ag layer. For the Ag/Si(111) system at 700°C the strain in the Ag layer would be much larger compared to that at RT. If we assume that this larger strain would be relaxed by introducing dislocations at the interface and a fully relaxed Ag layer would form at 700°C, the fully relaxed Ag layer would have  $d_{111}^{Ag} = 2.359\text{ Å}$ . As the thermal expansion coefficient of Ag is much higher than that of Si, in cooling the sample down to room temperature, the Ag layer would shrink at a higher rate than Si. As the in-plane Ag lattice would be pinned at the interface to that of Si, which shrinks at a slower rate, the Ag layer would have a larger shrinking in the surface-normal direction leading to a Ag(111) planar spacing in the surface-normal direction smaller than that of bulk Ag. This is schematically illustrated in Fig.11. A thick Ag layer is likely to undergo this process. This is

also consistent with the narrowness of the Ag(111) peak corresponding to the shorter  $d$ -spacing ( $d_{111}^{Ag} = 2.355\text{\AA}$ ). The lattice contraction is 0.17% with respect to the bulk  $d_{111}$  spacing. The weak broader Ag(111) peak is likely to be due to much thinner islands, which would be able to accommodate the strain due to thermal expansion mismatch without introducing dislocations. The presence of a thinner island is also seen in Fig.9(c). There are actually thin islands with a thickness variation. The broader peak corresponds to a lattice expansion of 0.21% compared to the bulk  $d_{111}$  spacing. For  $\lambda = 1.033\text{\AA}$ , the angular separation ( $\Delta\theta$ ) between the two Ag(111) peaks, as seen from Fig.10, is  $0.05^\circ$ . For  $\lambda = 0.709\text{\AA}$  this separation would be  $\Delta\theta = 0.03^\circ$  and with our laboratory set up it would be more difficult to observe these peaks as separated peaks.

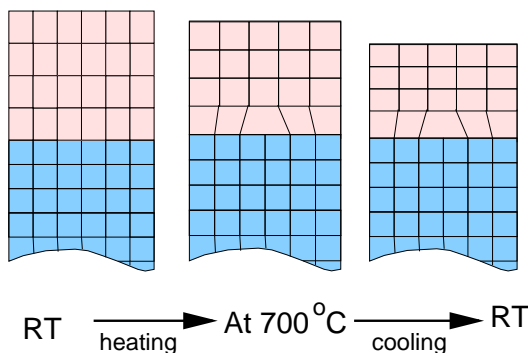


FIG. 11: The shortening of the perpendicular  $d$ -spacing in the annealed film compared to the corresponding bulk value is schematically illustrated. See text for details.

There are reports that desorption of Ag from a Ag/Si system starts around  $550^\circ\text{C}$  under UHV conditions [25]. Earlier we studied growth of Ag(111) layers ( $\sim 1000\text{\AA}$ ) on Si(111) and their annealing behavior under high vacuum (HV) condition by RBS/channeling experiments [21]. We have studied Ag/Si annealing (30 min) under high vacuum upto  $800^\circ\text{C}$ . At  $600^\circ\text{C}$ , we observed very little loss of Ag. At  $700^\circ\text{C}$  there were about 25% loss of Ag – mainly from grain boundaries without any detectable change of actual film thickness. At  $800^\circ\text{C}$  (30 min) Ag films were completely desorbed [26]. In the present case we expect that some desorption of Ag has taken place in the annealed film.

#### IV. SUMMARY AND CONCLUSIONS

We have studied growth of Ag on Si(111)-(7 $\times$ 7) surfaces at room temperature. Initial deposition of  $\sim 1$  ML Ag produces islands with a strongly preferred height of two atomic layers of Ag on the wetting layer. Thicker films show a tendency of growth of N-layer islands, where N is even. This appears to be a consequence of electron confinement in the metallic film. As-deposited thicker films ( $>20$  ML) show the formation of hexagonal islands at the top. These multi-tier islands have monatomic step edges. Annealed films show the formation of hexagonal disc-like islands. Individual islands show double-layer height at the edges, while multi-tier islands show monatomic height edges as in the as-deposited films. While the as-deposited films are epitaxial with a mosaic spread, the epitaxy improves up on annealing. An annealed 40 ML film has been found to show two closely-spaced Ag(111) peaks. The strong peak corresponding to shorter  $d$ -spacing compared to the bulk value can be explained by the perpendicular contraction up on cooling of the Ag lattice, which is presumably relaxed at high temperature during annealing, as a consequence of thermal expansion mismatch between Ag and Si.

Within our limited search we have not observed, for RT growth, any thickness window for the uniform layer growth – a prediction from the electronic growth mechanism. Obviously an extended search over film thickness and growth temperature would be necessary to explore this aspect.

The fact that bilayer growth is preferred even at the outer layers of relatively thick films needs further theoretical attention. Ag growth on Si(111)-(7 $\times$ 7) at RT cannot be simply classified within the three commonly known growth modes. The electronic confinement apparently plays a role in determining the film morphology. To what thickness electron confinement effect is operative is also an important aspect to be investigated.

#### V. ACKNOWLEDGEMENTS

We acknowledge the help provided by the HASYLAB staff. BND would like to thank Prof. J. R. Schneider for extending his support.

- 
- [1] Z. H. Zhang, S. Hasegawa and S. Ino, Phys. Rev. **B55**, 9983 (1997)
  - [2] K. R. Roos and M. C. Tringides, Surf. Sci. **302**, 37 (1994)
  - [3] G. Meyer and K. H. Rieder, Appl. Phys. Lett. **64**, 3560 (1994)
  - [4] For reviews, see J. A. Venables, Surf. Sci. **299/380**, 789 (1994); C. Argile and G. E. Rhead, Surf. Sci. Rep. **10**, 277 (1989)
  - [5] M. Hanbucken, M. Futamoto, and J. A. Venables, Surf.

- Sci. **147**, 433 (1984)
- [6] E. J. van Leenen, M. Iwami, R. M. Tromp and J. F. van der Veen, Surf. Sci. **137**, 1 (1984)
- [7] G. P. Chambers and B. D. Sartwell, Surf. Sci. **218**, 55 (1989)
- [8] L. Gavioli, K. R. Kimberlin, M. C. Tringides, J. F. Wendelken and Z. Zhang, Phys. Rev. Lett. **82**, 129 (1999)
- [9] Z. Y. Zhang, Q. Niu and C.-K. Shih, Phys. Rev. Lett. **80**, 5381 (1998)

- [10] Z. G. Suo and Z. Y. Zhang, Phys. Rev. **B58**, 5116
- [11] L. Huang, S. J. Chey and J. H. Weaver, Surf. Sci. **416**, L1101 (1998)
- [12] W. B. Su, S. H. Chang, W. B. Jian, C. S. Chang, L. J. Chen and T. T. Tsong, Phys. Rev. Lett. **86**, 5116 (2001)
- [13] H. Okamoto, D. Chen and T. Yamada, Phys. Rev. Lett. **89**, 256101-1(2002)
- [14] D. K. Goswami, B. Satpati, P. V. Satyam and B. N. Dev, Curr. Sci. **84**, 903 (2003)
- [15] D.-A. Luh, T. Miller, J. J. Paggel, M. Y. Chou and T.-C. Chiang, Science **292**, 1131 (2001)
- [16] C. M. Wei and M. Y. Chou, Phys. Rev. Lett. **68**, 125406 (2003); Phys. Rev. **B66**, 233408 (2002)
- [17] I. B. Altfeder, K. A. Matveev and D. M. Chen, Phys. Rev. Lett. **78**, 2815 (1997)
- [18] S. Liu, Z. Zhang, G. Comsa and H. Metiu, Phys. Rev. Lett. **71**, 2967 (1993)
- [19] W. J. Bartels, J. Hornstra and D. J. W. Lobeek, Acta. Cryst. **A42**, 539 (1986)
- [20] E. Z. Luo, S. Heun, M. Kennedy, J. Wollschlaeger and M. Henzler, Phys. Rev. **B49**, 4858 (1994)
- [21] B. Sundaravel, A. K. Das, S. K. Ghose, K. Sekar and B. N. Dev, Appl. Surf. Sci. **137**, 11 (1999) and references therein.
- [22] F. K. LeGoues, M. Liehr, M. Renier and W. Krakow, Philos. Mag. **B57**, 179 (1988)
- [23] A. Zur and T. C. McGill, J. Appl. Phys. **55**, 378 (1984)
- [24] <http://www.webelements.com>
- [25] S. Ino, T. Yamanaka and S. Ito, Surf. Sci. **283**, 319 (1983)
- [26] B. Sundaravel, A. K. Das, S. K. Ghose, B. Rout and B. N. Dev (unpublished)